Desalination and Water Treatment
www.deswater.com
doi: 10.5004/dwt.2020.25985

201 (2020) 155–164
October

Activated carbon derived from pistachio hull biomass for the effective removal of parabens from aqueous solutions: isotherms, kinetics, and free energy studies

Hamid Rashidi Nodeh[a,b], Hassan Sereshti[b,*], Sahar Ataolahi[b], Amirarshia Toloutehrani[b], Ali Talesh Ramezani[b]

[a]*Research Group of Food, Halal and Agricultural Products, Department of Food Industry and Agricultural Products, Standard Research Institute (SRI), Karaj, Iran, email: rnhamid2@gmail.com (H.R. Nodeh)*
[b]*School of Chemistry, College of Science, University of Tehran, Tehran, Iran, Tel. +98-21-66495291; Fax: +98-21-6113735; emails: sereshti@ut.ac.ir/sereshti@khayam.ut.ac.ir (H. Sereshti), tehraniarshia@ut.ac.ir (A. Toloutehrani), ali.tramezani75@ut.ac.ir (A. T. Ramezani)*

Received 20 October 2019; Accepted 16 April 2020

ABSTRACT

In this study, activated carbon biomass was prepared from pistachio hull (PiH-AC). The PiH-AC was used for removal of methylparaben (MP) and propylparaben (PP) from aqueous media. The biomass was fully characterized using Fourier transform-infrared spectroscopy, field emission-scanning electron microscopy, energy-dispersive X-ray spectroscopy, and Brunauer–Emmett–Teller surface morphology. The important parameters including pH of the solution, adsorbent dosage, ionic strength, contact time, initial solution concentration, and temperature were investigated. Furthermore, the process was fitted with adsorption isotherms, kinetics, and thermodynamic models to validate and predict the adsorption nature and mechanism. The Langmuir adsorption isotherm and pseudo-second-order kinetic models were best fitted to the experimental data. Langmuir isotherm was predicted monolayer pattern for selected parabens sorption with appropriate adsorption capacity of 55 and 50 mg g^{-1} for MP and PP, respectively. The value of free energy (E_a = ~2.45 kJ mol^{-1}) suggests a physisorption mechanism for selected parabens uptake onto the PiH-AC.

Keywords: Biomass; Pistachio hull activated carbon; Paraben; Equilibrium isotherm; Adsorption kinetics

1. Introduction

Parabens are formed as the result of a reaction between para-hydroxybenzoic acid with alkyl substituents ranging from methyl to butyl or benzyl groups, hence they are categorized into ester group [1,2]. They are widely used as preservatives in cosmetics, pharmaceuticals, foodstuff, and also industrial products that have been used for nearly 100 y due to their low cost, and broad spectrum of antimicrobial and anti-fungal properties [1,3,4]. Methylparaben and propylparaben are the most commonly used among the parabens and they often are present in the products together [1]. Because of their high consumption as a common preservative, parabens are present in environmental resources such as surface waters, soils, sediments and sludge, air, and dust and even have been detected in biota like fish tissue and also human tissue and body fluids [1,5]. Recent reports have indicated that extensive use of parabens may cause harm to human health. According to these reports, parabens play a role as endocrine disrupting agents, contribute

* Corresponding author.

to breast cancer, have an effect on male's reproductive system, trigger early onset of puberty, and also early aging [1,3,5]. In this regard, European Union (EU) and also food and drug administration (FDA), have recommended thresholds for using parabens as preservative: 0.4% for a single ester to be used and 0.8% for mixtures of all parabens in cosmetic products and also 1% in pharmaceutical products [1,5]. Parabens are continuously being released in urban wastewater at relatively high levels and despite being considerably removed during conventional sewage treatments, they are still being detected and reported in many aqueous media [4,6]. The presence of these compounds in wastewater may present a risk to human health. Thus, their removal from the environment is of the essence [7].

Various techniques have been applied for organic pollutants removal from water sources until now [8–12]. Methods such as photosensitized degradation [13], ozonation [14], and chlorine dioxide treatment [15] provide a high percentage of paraben removal but unfortunately, they produce disinfection by-products [4]. It seems among all methods, adsorption is a safer way and is the most suitable treatment for removing parabens from water and wastewaters [4,16]. It is a method that is free of harmful substances, environmentally friendlier, has a low initial costs, is flexible, and simple in design and operation [4,8,17]. In the adsorption process, choosing a suitable adsorbent is one of the most important steps. Activated carbon (AC) is known as an actual effective biomass adsorbent due to its microporous nature, large surface area, variable characteristics of surface chemistry, and high adsorption capacity [7,18–20]. AC can be synthesized from a wide variety of abundant and cheap with high carbon content and low inorganic content raw materials, [19,21]. Unfortunately, commercial AC is usually very expensive and suffers from impurities [7,19]. Therefore, in recent years, researchers focused on the biomass activated carbon preparation method based on agricultural waste and lignocelluloses materials which are more effective and also affordable [22–24]. A wide variety of agricultural and industrial waste are frequently used as AC precursor, such as corncob [25], hazelnut husk [26], olive stone [27], coconut shells [28], bamboo [29], rice husk [30], groundnut shell [31], pistachio-nut [32], and so forth [19,33]. There are two different processes to prepare activated carbon; chemical and physical treatment. Chemical activation requires oxidizing agents such as $ZnCl_2$, H_3PO_4, H_2SO_4, K_2S, NaOH, and KOH to be impregnated into the precursor and be washed to produce the activated carbon [33]. Hence, NaOH is an appropriate oxidizing agent due to its ability to produce carbon with a well-developed pore structure, less corrosion ability, and lower cost [7].

In this work, pistachio hull is used as the biomass activated carbon precursor as it is a carbon-rich source and it is free of cost. Hence, the present work describes the preparation and characterization of activated carbon (PiH-AC) from pistachio hulls in the presence of NaOH. Besides, the PiH-AC application was used to improve the removal of methylparaben and propylparaben from aqueous solutions. The main properties of the obtained PiH-AC, are high surface area, high porosity, possessing surface functional groups, and flake-like framework with PiH porous architecture.

2. Experimental

2.1. Chemicals and reagents

Raw pistachios were purchased from a local market and their hulls were used to prepare the activated carbon. Sodium hydroxide (NaOH), and hydrochloric acid (HCl) were purchased from Merck Chemicals (Darmstadt, Germany). Methylparaben and propylparaben were bought from SolarBio Co., (Beijing, China).

2.2. Preparation of activated carbon

At first, pistachios hull were completely dried at room temperature and then was powdered. Ten grams of this powder was mixed with 3 g of NaOH in 100 mL distilled water and was stirred for 24 h to remove lignans. The mixture was diluted and filtered via filter paper then washed with excess distilled water before drying in oven at 90°C. Thereafter, the dried powder was carbonized in a furnace at 410°C for 2 h. The obtained carbon was impregnated with NaOH solutions at a ratio of 3:1 (w/w) with 20 mL of distilled water and was stirred under magnetic stirring at 120°C for 1 h to get homogenous solution. Afterward, product was dried on heater at 140°C. Then, it was moved to the furnace and heated at 710°C for 2 h to complete the activation process. As the last step, AC sample was washed with HCl (0.01 M) and excess distilled water to be completely neutralize and was oven dried at 90°C for 24 h.

2.3. Apparatus

Surface morphology properties and elemental analysis of the raw materials and the activated carbon were investigated using a TESCAN MIRA3 (Prague, Czech Republic) field emission-scanning electron microscopy (FESEM) equipped with energy-dispersive X-ray spectroscopy (EDX). Specific surface area and pore diameter of the adsorbents were measured by the Belsorp-mini II BEL Japan Inc., (Osaka, Japan) under N_2 adsorption at 77 K. In order to remove moisture, the samples were outgassed at 373 K for 24 h. Functional groups of prepared activated carbon were identified by Bruker Equinox 55 Fourier transform-infrared spectroscopy (FT-IR) spectrometer (Bremen, Germany). IR spectra were recorded under transmission mode in the wavenumber ranged from 450 to 4,000 cm^{-1}. Concentration of parabens were determined by a Rayleigh-UV 2601 spectrophotometer (Beijing, China) in the range from 200 to 400 nm and lambda max (λ_{max}) at 260 nm.

2.4. Adsorption procedure

At first, a solution of methylparaben (MP) and propylparaben (PP) in water (20 mg L^{-1}) was prepared. Then, 20 mg of activated carbon was added into the solution. Effective parameters of the adsorption performance were investigated by varying pH of the solution (2–10), the mass of activated carbon (10–100 mg), NaCl salt (0–10%, w/v), adsorption time (10–300 min), initial concentration of MP and PP (10–300 mg L^{-1}), and solution temperature (25°C–50°C). After each adsorption procedure, the adsorbent was separated from water sample by filter paper.

The aliquot amount of supernatant was filtered through 0.45 μm PTFE syringe filter and then was transferred in a vial for determination of the residual concentration of MP and PP by UV-Vis spectrophotometer. The removal efficiency (R %) and equilibrium adsorption capacity (Q_e) were calculated using Eqs. (1) and (2), respectively.

$$(R\%) = \left(\frac{(C_0 - C_e)}{C_0}\right) \times 100 \quad (1)$$

$$Q_e = \frac{V}{m} \times (C_0 - C_e) \quad (2)$$

where Q_e is the equilibrium adsorption capacity (mg g^{-1}), C_0 is the initial concentration of parabens before adsorption (mg L^{-1}), C_e is the concentration of parabens after adsorption in water (mg L^{-1}), V is the aqueous solution volume (L), and m is the adsorbent dosage (g).

3. Results and discussion

3.1. Characterization

3.1.1. FT-IR spectroscopy

Fig. 1 shows the FT-IR spectra of the carbonized pistachio hull (A), and the home-made activated carbon (B). In Fig. 1a, the appearance of various transmittance bands in the wavenumber ranged from 3,370–1,124 cm^{-1} indicates the presence of functional groups in the carbonized material. The functional groups could be attributed to O–H stretching vibrations at 3,370 cm^{-1}, N–H stretching vibrations at 3,179 cm^{-1}, C–H stretching vibrations at 2,917 cm^{-1}, C=O axial deformation (carboxyl, ketone, or aldehyde groups), and the highly conjugated oxygen functional groups at 1,560 cm^{-1}, C–C stretching at 1,449 cm^{-1}, C–N stretching at 1,376 cm^{-1} and C–OH stretching at 1,124 cm^{-1} [34–36]. Following the activation of pistachio hull carbon at a high temperature some characteristics bands appear in IR spectra (Fig. 1b) at 3,432 cm^{-1} (O–H stretching), 2,921 cm^{-1} (C–H), 1,588 cm^{-1} (C=O) and 1,125 cm^{-1} (C–OH). As Fig. 1b illustrates, in the activated carbon there are less functional groups compared to the carbonized pistachio hull. This is probably due to breaking of some bands or decomposition of volatile compounds during the activation at high temperatures [34]. Figs. 1c and d represent the FT-IR spectra of parabens loaded adsorbent after adsorption process. As can be seen, extra IR bands are observed at 1,741 cm^{-1} (C=O), 1,284 cm^{-1} (C(O)–O stretching vibration), 1,211 cm^{-1} (O–H vibration), and 1,005 cm^{-1} (C–H vibration) for AC–PP and AC–MP as compared activated carbon (Fig. 1b).

3.1.2. Field emission scanning electron microscopy

Fig. 2a shows the SEM micrograph of the carbonized pistachio hull, in which micro-sized pore structures are observed. In the case of activation, nano-sized pores have been produced with high interconnected morphology (Fig. 2b). In the magnified micrograph (Fig. 2c), a three-dimensional flake like framework with a porous morphology less than 500 nm is observed. Besides, uniform flake sheets were observed with a thickness of approximately 30 nm for PiH-AC. However, successful synthesis of three-dimensional leaf-like activated carbon biomass was previously reported [37,38].

3.1.3. Specific surface area analysis (Brunauer–Emmett–Teller)

The specific surface area of the carbonized pistachio hull and PiH-AC was investigated based on nitrogen adsorption–desorption isotherm at 77 K [39], and the results are illustrated in Fig. 2d. The gas adsorption–desorption isotherm for PiH-AC follows the Type I pattern (set by IUPAC) at wide relative pressure (P/P_0) from 0 to 1 with R^2 = 0.9993. In contrast, the isotherm for carbonized pistachio hull does not follow the specific adsorption–desorption pattern. Based on the isotherms, the Brunauer–Emmett–Teller (BET) specific surface area and pore diameter are

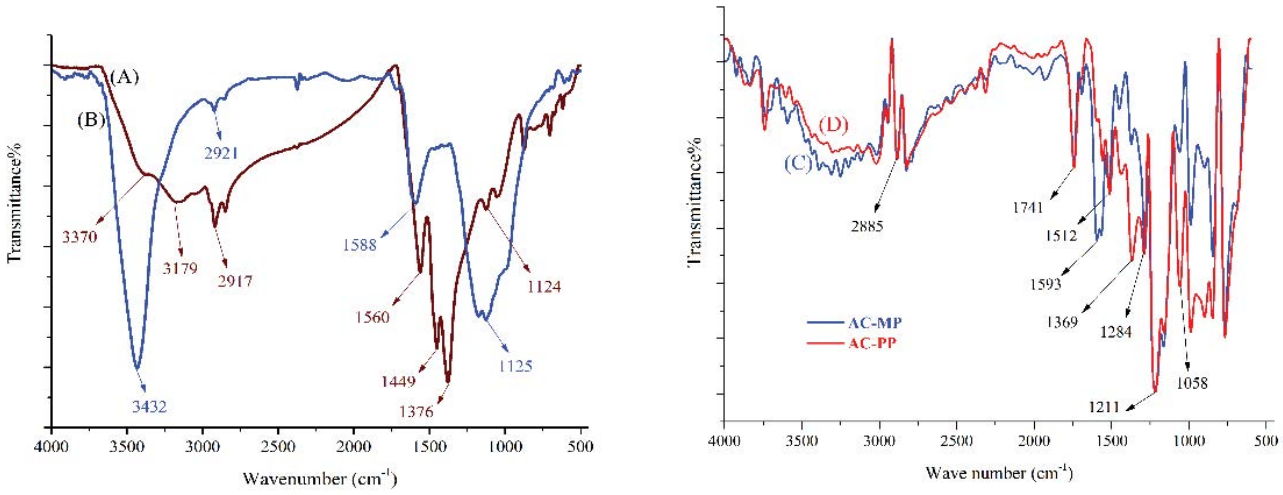

Fig. 1. FT-IR spectra of (a) carbonized pistachio hull and (b) activated carbon. After adsorption process of methyl paraben (c) and propyl paraben (d) loaded activated carbon.

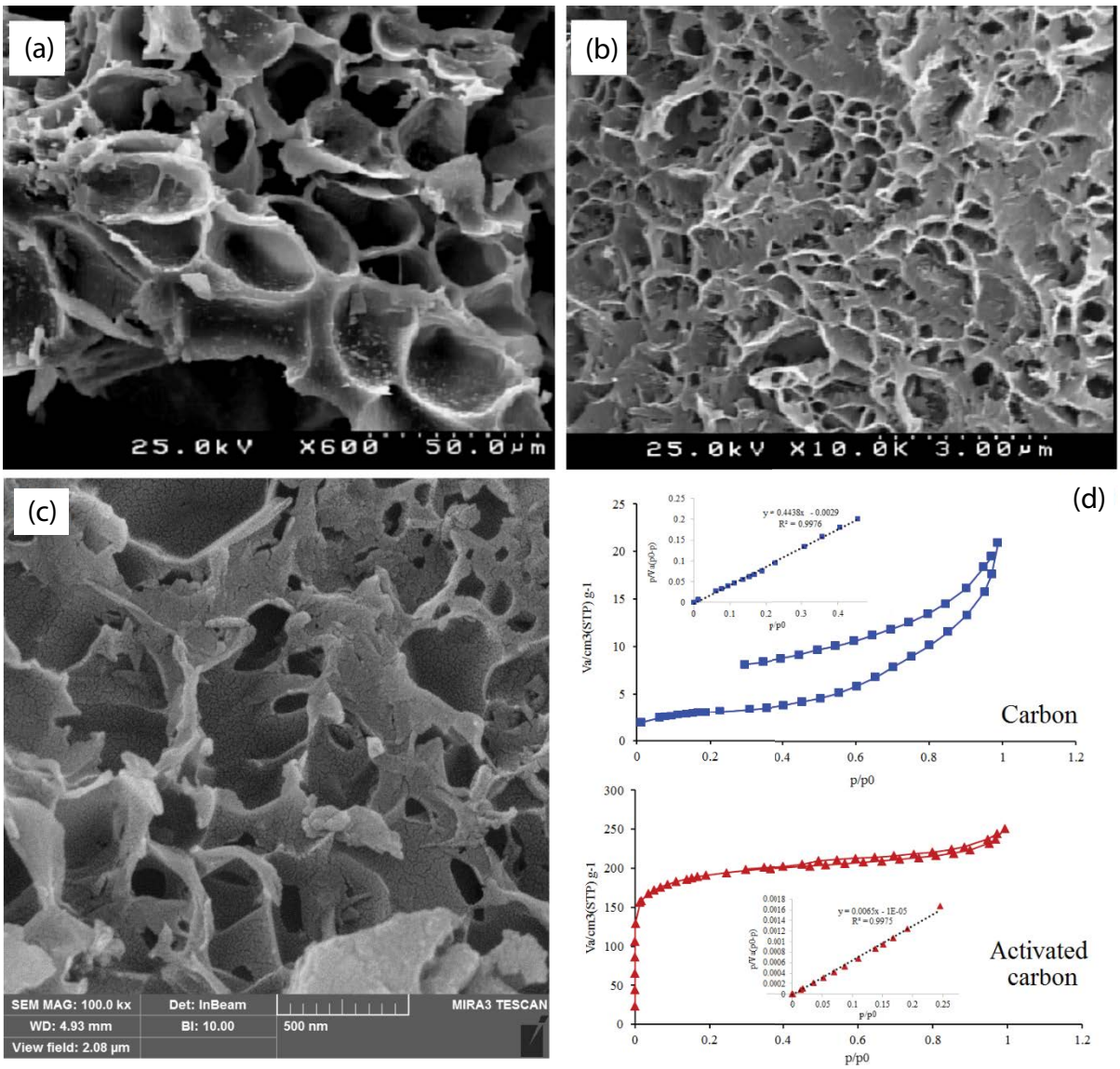

Fig. 2. FESEM micrographs of (a) carbonized pistachio hull at the magnification ×600, 50 µm, (b) porous activated carbon (PiH-AC) at the magnification ×10,000, 3 µm, and (c) PiH-AC at magnification ×100,000, 500 nm. (d) The BET analysis of the carbonized pistachio hull and PiH-AC.

9.64 m^2 g^{-1} (13.414 nm) and 457.77 m^2 g^{-1} (3.377 nm) for carbonized pistachio hull and PiH-AC, respectively. Additionally, these results indicate that the activation process significantly increased the surface area. Moreover, the activation process appropriately decreased the pore diameter to produce mesopores material. Mesopores materials with high surface area are more suitable to be used as an adsorbent material to enhance removal of various pollutant.

3.2. Effect of pH

The solution pH plays a significant role in adsorption process, as it can affect the chemical structure of analytes and also the surface charge of adsorbent [40,41]. Thus, the effect of this parameter on the parabens adsorption, was examined at different pHs (2, 4, 6, 8, and 10). Fig. 3a illustrates the effect of pH on the adsorption behavior of methylparaben (MP) and propylparaben (PP) onto the synthesized PiH-AC. As Fig. 3a shows, the highest adsorption efficiency was obtained at pH 4–6 for both selected parabens and afterward, it decreased gradually until pH 10. A survey in literature, shows that some mechanisms may take place in the adsorption process involving activated carbons, such as electrostatic interaction, hydrogen bonding formation, electron donor-acceptor, and π–π dispersion interaction [36]. According to electrostatic interaction theory, regarding the pK_a values of MP (8.17) and PP (8.35) [42], at high pHs, repulsion electrostatic interaction may happen between the adsorbent and parabens. Increasing pH promoted the deprotonation of parabens followed by the repulsion between the analyte and negatively charged adsorbent. The high adsorption at pH = 4–6

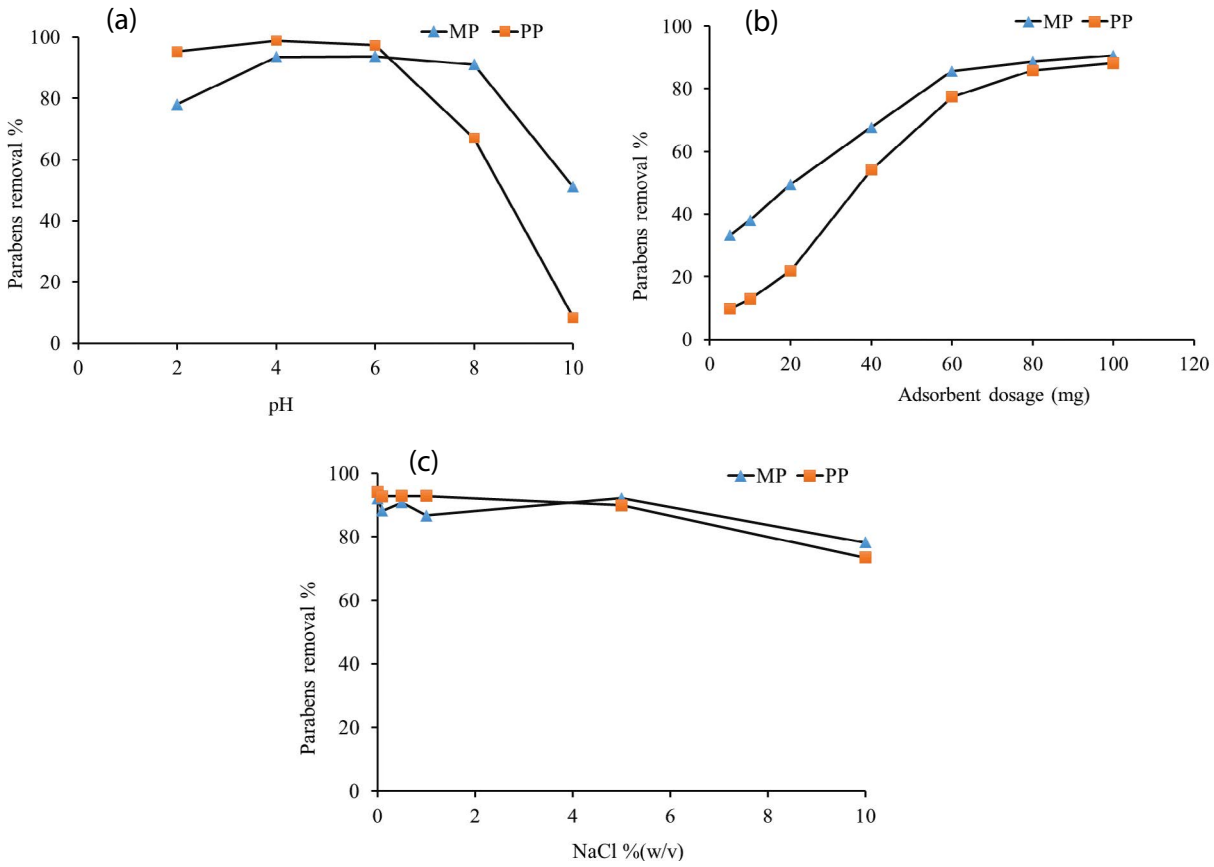

Fig. 3. Effect of (a) pH, (b) adsorbent dosage, and (c) salt concentration on the adsorption of parabens onto the activated carbon.

can be attributed to the maximum stability of parabens in this pH values through electrostatic interaction, hydrogen bonding formation and π–π interactions [43,44]. Thus, further experiments were performed at pH = 6.

3.3. Effect of adsorbent dosage

The effect of adsorbent dosage of methylparaben and propylparaben as another important parameter in adsorption were assessed by changing the mass of adsorbent in the range of 10–120 mg and the results are shown in Fig. 3b. According to that, the adsorption efficiency increased with an increase in the mass of adsorbent from 10 to 60 mg and after that remained almost constant. The reason probably is due to an increase in the number of available adsorption sites, and thus more analytes can occupy these sites, hence adsorption increases. But after that, it reached the adsorption equilibrium at 60–100 mg of adsorbent, so no sensible uptake was observed. Consequently, all the experiments were performed with a fixed mass of adsorbent, that is, 60 mg.

3.4. Effect of ionic strength

The salt concentration is another parameter that could affect the adsorption performance by changing ionic strength of the sample solution. The effect of salt concentration was studied by adding different amount of NaCl in the range of 0%–10% (w/v) into the sample solution prior to addition of adsorbent. According to data in the Fig. 3c, by increasing the NaCl concentration into the sample solution, the percentage of adsorption does not change dramatically. Therefore, as the salt has no effect on the adsorption of parabens on the activated carbon, further experiments were performed without adding salt.

3.5. Effect of contact time

The contact time is another key parameter in the adsorption process. To optimize the adsorption time, it was studied in the range from 10 to 300 min. According to Fig. 4a, as the contact time increases, adsorption increases too, and the reason is probably due to more contact time between analyte and adsorbent. As seen in Fig. 4a, the slope of the plot is high until 60 min and after that becomes milder and then almost constant as the equilibrium of reaction the between analytes and activated carbon comes close. Therefore, 60 min was chosen as the optimum time for parabens adsorption process.

3.6. Kinetic study

Adsorption rate between parabens and PiH activated carbon is described by sorption kinetic models namely

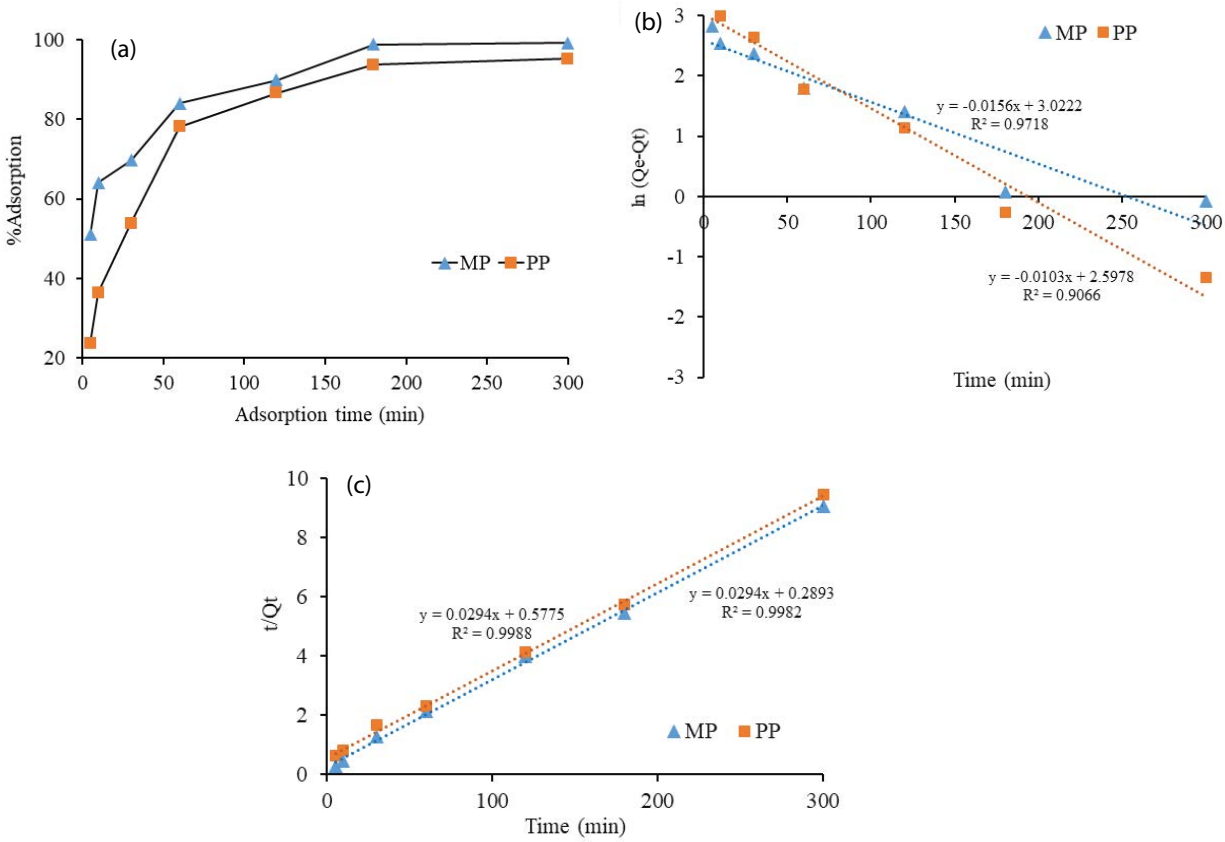

Fig. 4. (a) Effect of contact time on parabens adsorption. The kinetics of (b) pseudo-first-order, and (c) pseudo-second-order linear models.

pseudo-first-order and pseudo-second-order. These models are more appropriate to validate the experimental adsorption rate of parabens sorption onto the activated carbon. The Linear form of the proposed models is plotted by $\ln(Q_e - Q_t)$ vs. t and Q_t/t vs. t (Figs. 4b and c) and their values are expressed in Table 1. Table 1 illustrates parabens adsorption rate is well-described by pseudo-second-order due to high values of coefficient of determination (R^2 = 0.999). The small differences between Q_e (experimental) and Q_e (theory) in pseudo-second-order model suggests the adsorption rate may be limited through the exchange or sharing electrons between the adsorbent and the adsorbed [44,45].

3.7. Adsorption isotherm

Experiments on adsorption isotherm were conducted in order to determine the equilibrium adsorption capacity (Q_e, mg g^{-1}). Generally, adsorption isotherm describes the phenomenon governing the release or mobility of adsorbate from a liquid into solid adsorbent [41]. Hence, equilibrium was studied in different concentration of parabens in the range of 10–200 mg L^{-1} (20 mL), 40 mg adsorbent, and 180 min shaking time at pH 6. The values of Q_e (mg g^{-1}) was obtained from Eq. (2) and was plotted vs. C_e (mg L^{-1}) as shown in Fig. 5a. It is clear that the adsorption capacity was increased by the increase of the initial concentration until it reaches equilibrium. At high concentrations the adsorption system reaches equilibrium, this is probably due to saturation of adsorbent active cites [34,40].

Hence, in order to describe the nature of the adsorption equilibrium, isotherm models, Langmuir, Freundlich, and Dubinin–Radushkevich were investigated [46,47]. Additionally, the proposed isotherm models are able to describe the adsorption capacity, the adsorbed layer (pattern), and sorption mechanism (interaction) [41,48]. The values of isotherm parameters were calculated from linear equations (Table 2), by plotting C_e/Q_e vs. C_e (Langmuir), $\ln Q_e$ vs. $\ln C_e$ (Freundlich), and $\ln Q_e$ vs. ε^2 (Dubinin) as shown in Figs. 5c–f, respectively.

According to the value of R^2 of three isotherms (Table 2), the adsorption of parabens onto activated carbon follows the Langmuir model. This suggests a monolayer pattern of parabens sorption onto the activated carbon. In addition, the value of sorption free energy (E_a) indicates the paraben uptake of activated carbon follows physisorption mechanism. Since E_a values in the range of 1–8 kJ mol^{-1}, it suggests physisorption and 20–40 kJ mol^{-1} chemisorption mechanism for sorption process [44,49].

3.8. Regeneration and real sample analysis

In order to study the regeneration of the newly prepared activated carbon, the adsorption–desorption procedure was conducted several times. In this light, the loaded

Table 1
Kinetic rate models and their constants for adsorption of parabens onto the activated carbon

Model	Linear equation	Constant	Adsorbate	
			MP	PP
Pseudo-first-order	$\ln(Q_e - Q_t) = \ln Q_e - k_1 t$	Q_e (mg g^{-1})	13.09	20.11
		k_1 (min^{-1})	0.010	0.015
		R^2	0.971	0.906
Pseudo-second-order	$\frac{t}{Q_t} = \frac{1}{k_2 Q_e^2} + \frac{1}{Q_e}$	Q_e (mg g^{-1})	33.02	34.01
		k_2 (g mg^{-1} min^{-1})	0.0008	0.0008
		R^2	0.998	0.999

Table 2
Linear for of the Langmuir, Freundlich, and Dubinin–Radushkevich isotherm models and their constants for adsorption of parabens onto activated carbon

Model	Equation	Isotherm constant	Adsorbate	
			MP	PP
Langmuir	$\frac{C_e}{Q_e} = \frac{C_e}{Q_m} + \frac{1}{kQ_m}$	Q_m (mg g^{-1})	55.52	50.10
		k (L mg^{-1})	0.301	0.382
		R^2	0.997	0.998
Freundlich	$\ln q_e = \ln K_F + \left(\frac{1}{n}\right)\ln C_e$	K_F (mg g^{-1})	11.42	13.22
		n	3.33	3.03
		R^2	0.873	0.945
Dubinin–Radushkevich	$\ln q_e = \ln q_s - \left(K_{ad}\varepsilon^2\right)$	Q_s (mg g^{-1})	35.36	37.16
		K_{ad}	0.082	0.083
	$\varepsilon = RT\ln\left[1 + \frac{1}{C_e}\right]$	R^2	0.866	0.851
	$E_a = \left(2K_{ad}\right)^{-1/2}$	E_a (kJ mol^{-1})	2.46	2.45

parabens were desorbed from adsorbent using methanol (5 mL) for 10 min shaking on plate-shaker. Then, the removal percentage was calculated for the fifteenth continuous adsorption–desorption cycle. Hence, the activated carbon can be regenerated at least 15 times with high removal efficiency of 91.37% and 87.13% for MP and PP, respectively.

In further experiments, the prepared activated carbon was used for the removal of the selected parabens from wastewater samples. The aliquot concentration of parabens (20 mg L^{-1}) was added to wastewater sample and the removal process was conducted using activated carbon. The proposed adsorbent provided appropriate removal efficiency (>84%) for both of the selected parabens in complex matrix wastewater. These indicate that the PiH activated carbon is an efficient material for the removal of parabens residuals from wastewater media.

3.9. Comparison

The removal efficiency and adsorption capacity of the as-prepared PiH activated carbon and other materials were compared and listed in Table 3. The newly prepared PiH activated carbon provides high Q_e values for selected parabens compared to some other adsorbent, magnetic phenyl, polyacrylonitrile bead, and Fe_3O_4/$BiVO_4$. The results indicate the PiH activated carbon and β-cyclodextrin adsorbents are more suitable for parabens removal from aqueous media.

4. Conclusion

A novel porous activated carbon biomass derived from pistachio hull was successfully synthesized. The PiH-AC was characterized and applied to enhance the removal of MP and PP parabens from a water sample. The adsorption process was evaluated with isotherm models such as Langmuir, Freundlich, and Dubinin–Radushkevich isotherms. Due to the high value of R^2, Langmuir model was well-fitted to experimental data as compared to other models. Langmuir predicts high adsorption capacity for selected MP (55.52 mg g^{-1}) and PP (50.10 mg g^{-1}) parabens uptake using PiH-AC at pH 6. According to Langmuir isotherm, parabens adsorption process follows a monolayer pattern. According to the kinetic study, pseudo-second-order model was the best model to describe the experimental sorption rate. However, regarding the value of free energy

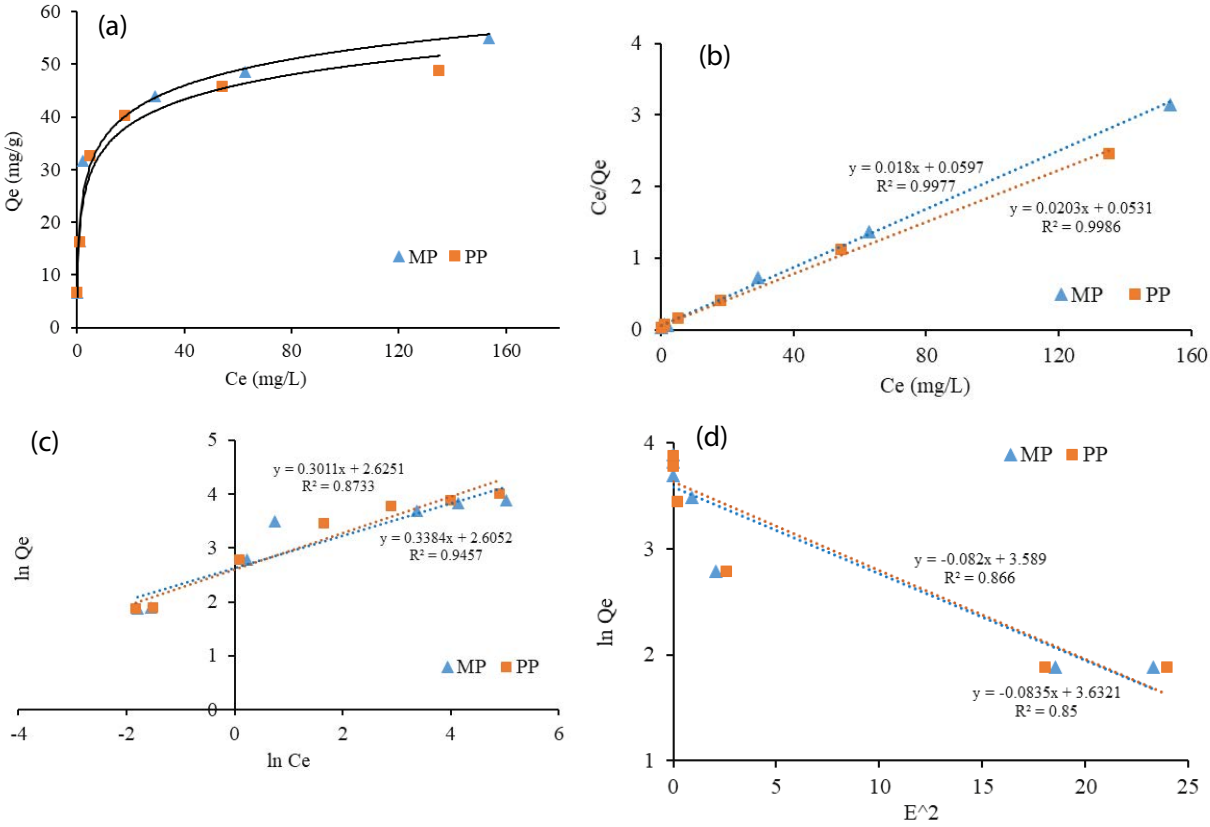

Fig. 5. (a) Experimental adsorption isotherm, (b) linear form of Langmuir model, (c) Freundlich linear model, and (d) Dubinin–Radushkevich isotherm.

Table 3
Comparison of parabens removal using different adsorbent

Adsorbent	Parabens	pH	Time (min)	Q_e (mg g^{-1})	Reference
PiH-activated carbon	MP, PP	6	120	55.52, 50.1	This study
β-cyclodextrin	MP, PP, EP, BP	–	120	15.2–60.5	[4]
Magnetic phenyl	MP, PP, EP	5	5	0.6–3.5	[8]
Polyacrylonitrile bead	MP	5.5	40	0.17	[44]
Fe_3O_4/$BiVO_4$	MP	5.3	120	97.40%	[37]

MP: methyl parabene, PP: propyl paraben, EP: ethyl parabene, BP: benzyl paraben.

(~2.45 kJ mol^{-1}) parabens uptake onto PiH-AC follows a physisorption mechanism. Particularly, the novelty of this work to prepare PiH-AC is utilizing inexpensive biomass for the efficient removal of parabens from environmental aqueous solutions.

References

[1] D. Błędzka, J. Gromadzińska, W. Wąsowicz, Parabens: from environmental studies to human health, Environ. Int., 67 (2014) 27–42.
[2] A. Mehdinia, M. Bahrami, S. Mozaffari, A comparative study on different functionalized mesoporous silica nanomagnetic sorbents for efficient extraction of parabens, J. Iran. Chem. Soc., 12 (2015) 1543–1552.
[3] C. Haman, X. Dauchy, C. Rosin, Occurrence, fate and behavior of parabens in aquatic environments: a review, Water Res., 68 (2015) 1–11.
[4] Y.P. Chin, S. Mohamad, M. Radzi, B. Abas, Removal of parabens from aqueous solution using β-cyclodextrin cross-linked polymer, Int. J. Mol. Sci., 11 (2010) 3459–3471.
[5] A.K. Srivastav, D. Dubey, D. Chopra, R.S. Ray, Toxicological potential of parabens – a widely used preservative, Global J. Multidiscip. Stud., 4 (2014) 1–5.
[6] B. Quintana, I. Rodrı, R. Cela, Evaluation of the occurrence and biodegradation of parabens and halogenated by-products in wastewater by accurate-mass liquid chromatography-quadrupole-time-of-flight-mass, Water Res., 5 (2011) 6770–6780.
[7] M.J. Ahmed, S.K. Theydan, Fluoroquinolones antibiotics adsorption onto microporous activated carbon from lignocellulosic biomass by microwave pyrolysis, J. Taiwan Inst. Chem. Eng., 45 (2014) 219–226.

[8] H. Chen, C. Chiou, S. Chang, Comparison of methylparaben, ethylparaben and propylparaben adsorption onto magnetic nanoparticles with phenyl group, Powder Technol., 311 (2017) 426–431.
[9] W. Chou, Y. Huang, Electrochemical removal of indium ions from aqueous solution using iron electrodes, 172 (2009) 46–53.
[10] H.M. Inamisawa, K.M. Urashima, M.M. Inamisawa, N.A. Rai, T.O. Kutani, Determination of indium by graphite furnace atomic absorption spectrometry after coprecipitation with chitosan, Anal. Sci., 19 (2003) 401–404.
[11] H. Ma, Y. Lei, Q. Jia, W. Liao, L. Lin, An extraction study of gallium, indium, and zinc with mixtures of sec-octylphenoxyacetic acid and primary amine N1923, Sep. Purif. Technol., 80 (2011) 351–355.
[12] R.D. Ambashta, M. Sillanpää, Water purification using magnetic assistance : a review, J. Hazard. Mater., 180 (2010) 38–49.
[13] D. Gryglik, J.S. Miller, The aqueous photosensitized degradation of butylparaben, Photochem. Photobiol. Sci., 8 (2009) 549–555.
[14] K. Soo Tay, N.A. Rahman, M.R.B. Abas, Kinetic studies of the degradation of parabens in aqueous solution by ozone oxidation, Environ. Chem. Lett., 4 (2009) 331–337.
[15] H.R. Andersen, E. Eriksson, Estrogenic personal care products in a greywater reuse system, Water Sci. Technol., 56 (2007) 45–49.
[16] I. Márquez-Sillero, E. Aguilera-Herrador, S. Cárdenas, M. Valcárcel, Determination of parabens in cosmetic products using multi-walled carbon nanotubes as solid phase extraction sorbent and corona-charged aerosol detection system., J. Chromatogr. A, 1217 (2010) 1–6.
[17] I. Ali, New generation adsorbents for water treatment, Chem. Rev., 112 (2012) 5073–5091.
[18] T.M. Alslaibi, I. Abustan, M.A. Ahmad, A. Foul, A review: production of activated carbon from agricultural byproducts via conventional and microwave heating, J. Chem. Technol. Biotechnol., 88 (2013) 1183–1190.
[19] J.M. Dias, M.C.M. Alvim-ferraz, M.F. Almeida, M. Sa, Waste materials for activated carbon preparation and its use in aqueous-phase treatment: a review, J. Environ. Manage., 85 (2007) 833–846.
[20] K.A. Krishnan, K.G. Sreejalekshmi, V. Vimexen, V.V Dev, Evaluation of adsorption properties of sulphurised activated carbon for the effective and economically viable removal of Zn(II) from aqueous solutions, Ecotoxicol. Environ. Saf., 124 (2016) 418–425.
[21] W. Liu, H. Yuan, Characterization and application of activated carbon regenerated by the combination of sulfuric acid pretreatment and thermal regeneration, Desal. Water Treat., 178 (2020) 83–93.
[22] M. Rezvani, G. Najafpou, M. Mohammadi, H. Zare, Amperometric biosensor for detection of triglyceride tributyrin based on zero point charge of activated carbon, Turk. J. Biol., 41 (2017) 268–277.
[23] R. Mailler, J. Gasperi, Y. Coquet, A. Buleté, E. Vulliet, S. Deshayes, S. Zedek, C. Mirande-Bret, V. Eudes, A. Bressy, Removal of a wide range of emerging pollutants from wastewater treatment plant discharges by micro-grain activated carbon in fluidized bed as tertiary treatment at large pilot scale, Sci. Total Environ., 542 (2016) 983–996.
[24] S. Mohammad, D.E. Abulyazied, S.M. Ahmed, Application of polyaniline/activated carbon nanocomposites derived from different agriculture wastes for the removal of Pb(II) from aqueous media, Desal. Water Treat., 170 (2019) 199–210.
[25] S. Nethaji, A. Sivasamy, A.B. Mandal, Bioresource technology preparation and characterization of corn cob activated carbon coated with nano-sized magnetite particles for the removal of Cr(VI), Bioresour. Technol., 134 (2013) 94–100.
[26] G. Karaçetin, S. Sivrikayaa, M. Imamoğlu, Adsorption of methylene blue from aqueous solutions by activated carbon prepared from hazelnut husk using zinc chloride, J. Anal. Appl. Pyrolysis. 110 (2014) 270–276.
[27] L. Limousy, I. Ghouma, A. Ouederni, M. Jeguirim, Amoxicillin removal from aqueous solution using activated carbon prepared by chemical activation of olive stone, Environ. Sci. Pollut. Res. Int., 24 (2016) 9993–10004.
[28] R.R. Karri, N.S. Jayakumar, J.N. Sahu, Modelling of fluidised-bed reactor by differential evolution optimization for phenol removal using coconut shells based activated carbon, J. Mol. Liq., 231 (2017) 249–262.
[29] M. Fujishige, I. Yoshida, Y. Toya, Y. Banba, K. Oshida, Y. Tanaka, P. Dulyaseree, W. Wongwiriyapan, K. Takeuchi, Preparation of activated carbon from bamboo-cellulose fiber and its use for EDLC electrode material, J. Environ. Chem. Eng., 5 (2017) 1801–1808.
[30] A. Mullick, S. Moulik, S. Bhattacharjee, Removal of hexavalent chromium from aqueous solutions by low-cost rice husk-based activated carbon: kinetic and thermodynamic studies, Indian Chem. Eng., 1 (2017) 1–14.
[31] M. Kamaraj, P. Umamaheswari, Preparation and characterization of groundnut shell activated carbon as an efficient adsorbent for the removal of Methylene blue dye from aqueous solution with microbiostatic activity, J. Mater. Environ. Sci., 8 (2017) 2019–2025.
[32] F.T. Foroushani, H. Tavanai, F.A. Hosseini, Microporous and mesoporous materials an investigation on the effect of $KMnO_4$ on the pore characteristics of pistachio nut shell based activated carbon, Microporous Mesoporous Mater., 230 (2016) 39–48.
[33] M. Adib, Z. Al-qodah, C.W.Z. Ngah, Agricultural bio-waste materials as potential sustainable precursors used for activated carbon production: a review, Renewable Sustainable Energy Rev., 46 (2015) 218–235.
[34] K.C. Bedin, A.C. Martins, A.L. Cazetta, O. Pezoti, V.C. Almeida, KOH-activated carbon prepared from sucrose spherical carbon: adsorption equilibrium, kinetic and thermodynamic studies for Methylene blue removal, Chem. Eng. J., 286 (2016) 476–484.
[35] O. Pezoti, A.L. Cazetta, K.C. Bedin, L.S. Souza, A.C. Martins, T.L. Silva, O.O.S. Júnior, J.V Visentainer, V.C. Almeida, NaOH-activated carbon of high surface area produced from guava seeds as a high-efficiency adsorbent for amoxicillin removal: kinetic, isotherm and thermodynamic studies, Chem. Eng. J., 288 (2016) 778–788.
[36] A.C. Martins, O. Pezoti, A.L. Cazetta, K.C. Bedin, D.A.S. Yamazaki, G.F.G. Bandoch, T. Asefa, J.V Visentainer, V.C. Almeida, Removal of tetracycline by NaOH-activated carbon produced from macadamia nut shells: kinetic and equilibrium studies, Chem. Eng. J., 260 (2015) 291–299.
[37] K. Ojha, B. Kumar, A.K. Ganguli, Biomass derived graphene-like activated and non-activated porous carbon for advanced supercapacitors, J. Chem. Sci., 129 (2017) 397–404.
[38] L. Zhou, T. Huang, A. Yu, Three-dimensional flower-shaped activated porous carbon/sulfur composites as cathode materials for lithium–sulfur batteries, ACS Sustainable Chem. Eng., 2 (2014) 2442–2447.
[39] K. Le Van, T.T.L. Thi, Activated carbon derived from rice husk by NaOH activation and its application in supercapacitor, Prog. Nat. Sci. Mater. Int., 24 (2014) 191–198.
[40] H. Rashidi Nodeh, H. Sereshti, Synthesis of magnetic graphene oxide doped with strontium titanium trioxide nanoparticles as a nanocomposite for the removal of antibiotics from aqueous media, RSC Adv., 6 (2016) 89953–89965.
[41] M.A. Kamboh, W.A. Wan Ibrahim, H. Rashidi Nodeh, M.M. Sanagi, S.T.H. Sherazi, The removal of organophosphorus pesticides from water using a new amino-substituted calixarene-based magnetic sporopollenin, New J. Chem., 40 (2016) 3130–3138.
[42] C. Song, H. Hu, H. Ao, Y. Wu, C. Wu, Removal of parabens and their chlorinated by-products by periphyton: influence of light and temperature, Environ. Sci. Pollut. Res., 24 (2017) 5566–5575.
[43] J.-C.E. Yang, H. Lan, X.-Q. Lin, B. Yuan, M.-L. Fu, Synthetic conditions-regulated catalytic oxone efficacy of MnO_x/SBA-15 towards butyl paraben (BPB) removal under heterogeneous conditions, Chem. Eng. J., 289 (2016) 296–305.
[44] M. Forte, L. Mita, R. Perrone, S. Rossi, M. Argirò, D.G. Mita, M. Guida, M. Portaccio, T. Godievargova, Y. Ivanov, Removal of methylparaben from synthetic aqueous solutions using

polyacrylonitrile beads: kinetic and equilibrium studies, Environ. Sci. Pollut. Res., 24 (2017) 1270–1282.
[45] X. You, C. Piao, L. Chen, Preparation of a magnetic molecularly imprinted polymer by atom-transfer radical polymerization for the extraction of parabens from fruit juices, J. Sep. Sci., 39 (2016) 2831–2838.
[46] K. Singh, D.H. Lataye, K.L. Wasewar, Removal of fluoride from aqueous solution by using bael (*Aegle marmelos*) shell activated carbon: kinetic, equilibrium and thermodynamic study, J. Fluorine Chem., 194 (2017) 23–32.
[47] M.E. Bidhendia, M.A. Gabris, V. Goudarzi, S. Abedyni, B.H. Juma, H. Sereshtib, M.A. Kamboh, M. Soylak, H.R. Rashidi Nodeh, Removal of some heavy metal ions from water using novel adsorbent based on iron oxide-doped sol–gel organic-inorganic hybrid nanocomposite: equilibrium and kinetic studies, Desal. Water Treat., 147 (2019) 173–182.
[48] H. Rashidi Nodeh, H. Sereshti, E. Zamiri Afsharian, N. Nouri, Enhanced removal of phosphate and nitrate ions from aqueous media using nanosized lanthanum hydrous doped on magnetic graphene nanocomposite, J. Environ. Manage., 197 (2017). 265–274.
[49] S.S. Tahir, N. Rauf, Removal of a cationic dye from aqueous solutions by adsorption onto bentonite clay, Chemosphere, 63 (2006) 1842–1848.